# Моделирование траектории полёта винтовочной пули калибра 7,62 мм/0,308 дюйма путём численного решения уравнений движения материальной точки

Soham Gangopadhyay, Richa Rohatgi

National Institute of Criminology and Forensic Science, New Delhi, India

**АННОТАЦИЯ**

*Обоснование.* Для точной оценки различных переменных полёта снаряда в баллистике важно понимание динамики его траектории. Статья посвящена изучению фундаментальных принципов внешней баллистики, что позволяет рассмотреть характеристики траектории свободного полёта пуль калибра 0.308 дюйма через численное решение уравнений движения материальной точки.

*Цели исследования* — наблюдение за изменением коэффициента лобового сопротивления ($C_D$) в зависимости от числа Маха ($Ma$) и высоты полёта, а также вычисление среднего $C_D$ для каждой рассматриваемой пули; решение уравнений траектории движения материальной точки с тремя степенями свободы для заданных пуль, включая наблюдение за воздействием продольной составляющей баллистического ветра на поведение траектории в качестве переменной и аппроксимацией траектории полёта при настильной стрельбе под воздействием бокового ветра.

*Материал и методы.* Моделирование траекторий свободного полёта семи различных пуль винтовочного патрона калибра 7,62 мм/0,308 дюйма (B0–B6) выполняли путём численного решения уравнений движения. Средние коэффициенты $C_D$ для пуль B0–B6 вычисляли при помощи масштабирования вариаций $C_D$ в зависимости от числа Маха полёта относительно стандартного снаряда формы G7. Модель траектории движения материальной точки и аппроксимацию при настильной стрельбе изучали с/без учёта продольного ветра. Решение систем уравнений выполнено посредством написания скриптов на языке программирования Python и использования библиотеки Matplotlib для построения графиков смоделированных траекторий.

*Результаты.* Отмечено, что увеличение веса пули и, соответственно, поперечной нагрузки снижает $C_D$. Как и ожидалось, пуля с наибольшим лобовым сопротивлением (B0) имеет наименьшую дальность полёта и самую низкую высоту в апогее, тогда как пули с меньшим лобовым сопротивлением летят дальше и выше. Пересечение траекторий наблюдается при угле возвышения оружия ~30°, из чего следует, что максимальная дальность не достигается при стрельбе под углом 45°, как в случае с траекториями в безвоздушном пространстве. Для наблюдения за траекториями полёта и отклонением пуль при боковом ветре выполнена аппроксимация модели движения материальной точки при настильной стрельбе под углами возвышения менее 5°.

*Заключение.* В работе представлено численное решение уравнений движения материальной точки для пули винтовочного патрона с целью компьютерного моделирования её траектории. В качестве образцов для моделирования траекторий свободного полёта была выбрана группа из семи пуль калибра 7,62 мм/0,308 дюйма. Язык программирования Python хорошо подходит для численного решения систем дифференциальных уравнений благодаря библиотеке встроенных функций, с помощью которой можно написать эффективный скрипт и снизить вычислительную нагрузку. Такой метод решения может быть применён с соответствующими модификациями в области судебной баллистики для реконструкции траекторий пуль и формирования заключения на основе имеющихся улик с места преступления.

**Ключевые слова:** баллистический коэффициент; коэффициент лобового сопротивления; Python; материальная точка; настильная стрельба; траектории.

# Trajectory simulations by the numerical solution of the point-mass equations of motion for 7.62 mm/.308" rifle bullets

Soham Gangopadhyay, Richa Rohatgi

National Institute of Criminology and Forensic Science, New Delhi, India

### ABSTRACT

**BACKGROUND:** The understanding of the dynamics of the trajectory is important in ballistics to estimate the values of various flight variables accurately. The paper deals with the study of the fundamental principles of external ballistics, which allows to delve into the trajectory characteristics of the free flight trajectory of seven. 308" caliber bullets by numerically solving the point-mass equations of motion. Numerical solutions were performed by writing scripts in the Python programming language and using the Matplotlib library to plot simulated trajectories.

**AIM:** the three aims of the study were to observe the variation of $C_D$ with Mach number (*Ma*) of flight and calculate an average $C_D$ for each bullet under consideration. Further, solving the 3-DoF (Degrees-of-Freedom) Point-Mass trajectory equations of motion for the given bullets (along side observing the effects of range winds on the trajectory behaviour as a variable). And finally, solving the flat-fire approximation with analysis of the effects of a crosswind.

**MATERIALS AND METHODS:** Simulations of free-flight trajectories of seven different 7.62 mm/.308" rifle bullets (designated B0–B6) have been carried out by the numerical solution of the equations of motion. The average drag force coefficients ($C_D$) for B0–B6 have been calculated by scaling the variation of $C_D$ with the Mach number of flight with reference to the G7 standard projectile. The Point-Mass trajectory model and its Flat-Fire approximation have been studied with and without the effect of range winds. The solutions of the systems of equations have been carried out by writing scripts in the Python programming language.

**RESULTS:** It is observed that an increase in the bullet weight and consequently the sectional density lowers the $C_D$. As expected, it is seen that the bullet with the highest drag (B0) has the shortest range and lowest apogee, while lower drag bullets fly further and higher. The crossover of trajectories is observed at ~30° angle of gun elevation, which implies that the maximum range is not achieved when fired at 45°, as is the case with vacuum trajectories. Flat-fire approximation of the point-mass model was also solved to observe trajectories and crosswind deflections of the bullets when fired at <5° angles of elevation.

**CONCLUSION:** This project presents the numerical solution of equations of motion of the Point-Mass model for a bullet fired from a gun to computationally simulate its trajectory. A group of seven 7.62 mm/.308" rifle bullets were chosen as samples to simulate free-flight trajectories. The programming language Python is well-equipped to carry out numerical solutions of systems of differential equations owing to its library of in-built functions which assists in writing an efficient script and reduces computational load. This method of solution can be applied with suitable modifications in the field of forensic ballistics for the reconstruction of bullet trajectories and to form a conclusion based on the available evidence from a crime scene.

**Keywords:** ballistic coefficient; drag coefficient; Python; point-mass; flat-fire; trajectories.

# 通过求解质点运动方程的数值进行7.62毫米/0.308英寸步枪子弹的弹道模拟

Soham Gangopadhyay, Richa Rohatgi

National Institute of Criminology and Forensic Science, New Delhi, India

**简评**

**背景**：在弹道学中，了解弹道动力学对于精确估计各种飞行变量的数值非常重要。本文研究外弹道的基本原理，通过求解质点运动方程的数值，深入研究7颗0.308英寸口径子弹的自由飞行弹道的弹道特性。通过用Python编程语言编写脚本并使用Matplotlib库绘制模拟弹道来进行数值求解。

**目的。**该研究的三个目的是观察CD随飞行马赫数（Ma）的变化，并计算每颗子弹的平均$C_D$。此外，求解给定子弹的三自由度（3-DoF）质点弹道运动方程（同时观察射程风作为变量对弹道行为的影响）。最后，通过分析侧风的影响来求解平射近似。

**材料和方法**：通过数值求解运动方程模拟七颗不同的7.62毫米/0.308英寸步枪子弹（指定为B0–B6）的自由飞行弹道。    参照G7标准弹，计算B0–B6的平均阻力系数（$C_D$）随飞行马赫数的变化。    在分别受以及不受射程风影响的情况下，研究质点弹道模型及其平射近似。用Python编程语言编写的脚本进行方程组求解。

**结果。**观察发现，子弹重量的增加以及因此导致的截面密度的增加使CD降低。正如预期的那样，可以看出，阻力最大的子弹（B0）射程最短，远地点最低，而阻力越小的子弹飞得越高越远。在枪仰角约30°时观察到弹道交叉，这意味着以45°角射击时无法达到最大射程，这与真空弹道相符。质点模型的平射近似也得以解决，以观察子弹在<5°仰角下发射时的弹道和侧风偏转。

**结论。**本项目提出了通过求解从步枪发射的子弹的质点模型运动方程的数值，对其弹道进行计算模拟。选择了一组7颗7.62毫米/0.308英寸的步枪子弹为样本，模拟其自由飞行弹道。由于编程语言Python内置的函数库有助于编写高效脚本并减少计算负载，Python能够很好地执行微分方程组的数值解。该解决方法可以在适当修改后，应用于法医弹道学重建子弹弹道，并根据犯罪现场的可用证据得出结论。

**关键词**：弹道系数，阻力系数，Python，质点，平射，轨迹。

# BACKGROUND

The modern word 'Ballistics' has roots in the Greek word 'βαλλειν', meaning 'to throw'. The modern meaning of ballistics encompasses the motion of bodies projected at far greater velocities than human physiology can allow. These projectiles are propelled by the force of combustion of gunpowder or other solid fuel compounds, moving under the forces of gravity and other forces due to the projectile's shape and motion. A gun, or a firearm, is essentially a heat engine of Victorian design [1]. The source of thrust is the conversion of the chemical energy stored in the gunpowder, which is converted into heat upon combustion. The barrel is the cylinder through which the rapidly expanding gases push on the base of the bullet (the piston in the heat engine analogy), while the breech/bolt remains locked against the reactive force of the cartridge case. Modern ammunition is a self-contained round comprising of the powder, projectile and the primer in a brass/steel/plastic case. These rounds can be loaded individually into the chamber by the shooter or automatically loaded from a magazine, which feeds the gun. The flight of the bullet from the point it leaves the muzzle of the gun until it impacts upon the target is studied under exterior ballistics. The correct mathematical modelling of the bullet trajectory is necessary to correctly describe the flight of the spinning projectile in varying complexities. To estimate the values of various flight variables accurately, the understanding of the dynamics of the trajectory is important in ballistics.

Forensic science is defined as the application of scientific investigation of available evidence for the assistance in legal proceedings. Forensic ballistics involves the analysis of evidence gathered in crime scenes where there has been a discharge of one or more firearms. In investigation of crimes involving gun shots, it is important for the expert to have knowledge of basic ballistic behaviour of bullets regarding the range, time of flight, the angle and attitude of impact and the velocity of impact of the bullets fired from different guns. Different muzzle velocities and angles of firing result in trajectories that vary in height, range and shape for bullets of different calibres and constructions.

The present work reports a study of the fundamental principles of exterior ballistics, which will delve into the trajectory characteristics of the free flight of a rifle bullet. The results of the present work will contribute to the body of knowledge of forensic ballistics for the analysis of evidence in a shooting incident and for the formation of opinion regarding a case by the forensic expert. The data about flight characteristics of various bullets can assist in the process of crime scene reconstruction at the scene of crime or in the laboratory for estimating the position of the shooter, the angle of firing and the type of firearm used.

**Aim of the study:** Write Python scripts for the numerical solution of systems of differential equations; Observe the variation of $C_D$ with Mach number (*Ma*) of flight and calculate an average $C_D$ for each bullet under consideration; Use the average $C_D$ as an input for solving the 3-DoF (Degrees-of-Freedom) Point-Mass trajectory equations of motion for the given bullets, along with observation of the effects of range winds on the trajectory behaviour; Solution of the flat-fire approximation with analysis of the effects of a crosswind.

# MATERIALS AND METHODS
## Study design

The present work is a report of the study of the free-flight trajectory of seven bullets of .308" calibre by the numerical solution of the point-mass equations of motion. The numerical solutions have been carried out by writing scripts in the Python programming language and using the *matplotlib* library to plot the simulated trajectories.

## Methods

*Bullet Data.* Seven bullets have been chosen for observation. All the bullets have a calibre of 7.62 mm or .308", but they vary in weight and construction. The following table gives the physical data of the bullets (Table 1).

*Aerodynamic Drag Coefficient.* The drag coefficient has been estimated by using the experimentally measured Ballistic coefficients published by Sierra Bullets for their bullets [10]. The Ballistic Coefficient (BC) from live firings of a bullet can be calculated by measuring the near and far velocities of the bullet by velocity measurement systems placed a standard distance apart [11, 12]. The space function S(V) values which can be read out from the standard reference projectile firing table are then used to calculate the BC of the given bullet by,

$$BC = \frac{X}{S(v) - S(V)},$$

where $X$ = distance between velocity measurement systems; $V$ = muzzle velocity, or near velocity; $v$ = remaining velocity, or far velocity; *(V)*, *S(v)* = Space function values of the corresponding velocities.

Sierra bullets presents BC values in velocity bands since the form factor changes with velocity/Mach number of flight. The BC is calculated as,

$$BC = \frac{w/7000}{d^2 i} \left(\frac{lbs}{in^2}\right),$$

where $w$ = weight of the bullet (grains); $d$ = reference diameter (calibre); $i$ = form factor.

From which we get,

$$i = \frac{w/7000}{d^2 . BC}.$$

**Table 1.** Data of bullets B0 to B6 chosen for trajectory analysis

| Sl. No. | Bullet | | | | Image | Ballistic Coefficient Data | |
|---|---|---|---|---|---|---|---|
| | Designation | Nomenclature | Reference | Weight (grains) | | | |
| 1 | B0 | 7.62 mm Ball M80 | [2; 3 p. 62] | 147 |  | ≤1700 fps<br>1700–2500 fps<br>≥2500 fps | 0.197<br>0.200<br>0.205 |
| 2 | B1 | FMJBT #2115 | [4] | 150 |  | ≤1800 fps<br>1800–2800 fps<br>≥2800 fps | 0.387<br>0.397<br>0.408 |
| 3 | B2 | HPBT #2190 | [5] | 150 |  | ≤1800 fps<br>1800–2800 fps<br>≥2800 fps | 0.355<br>0.397<br>0.417 |
| 4 | B3 | SBT #2125 | [6] | 150 |  | ≤1800 fps<br>1800–2800 fps<br>≥2800 fps | 0.360<br>0.368<br>0.380 |
| 5 | B4 | SBT #2145 | [7] | 165 |  | ≤1600 fps<br>1600–2400 fps<br>≥2400 fps | 0.419<br>0.409<br>0.404 |
| 6 | B5 | TMK #2200 | [8] | 168 |  | ≤1650 fps<br>1650–2050 fps<br>≥2050 fps | 0.480<br>0.521<br>0.535 |
| 7 | B6 | HPBT #2275 | [9] | 175 |  | ≤1800 fps<br>1800–2800 fps<br>≥2800 fps | 0.485<br>0.496<br>0.505 |

The form factor thus calculated gives the ratio of the actual bullet drag coefficient $C_D$ to that of the standard ($C_{Dref}$) with a similar shape for the velocity range over which the BC is measured [13, 14].

$$i = \frac{C_D}{C_{D_{ref}}}.$$

The variation of the $C_D$ with *Ma* of the G7 projectile used as the reference for calculating the coefficient of drag for the bullets under consideration is given below (Table 2).

***The Point-Mass Trajectory Model.*** The 3-DoF Point-Mass model of projectile motion considers just the earth-fixed coordinate system (x, y, z), hence, the three degrees of freedom. The entire mass distribution of the bullet is assumed to be concentrated at a point, which negates the analysis of the orientation of the bullet body with respect to the velocity vector/trajectory. The simplest model of projectile motion is a point-mass vacuum trajectory. The vacuum trajectory does not take into account any forces acting on the projectile to retard it, except the gravitational attraction pulling it towards the ground. The vacuum trajectory is a combined motion of uniform horizontal translation and gravity accelerated vertical motion, and was first stated mathematically in its correct form by Galileo. However, though simple to describe and solve for a trajectory the vacuum trajectory can only be an approximation of actual motion of a projectile, especially for light bullets moving at high velocities. The vacuum trajectory provides a good approximation for slow-moving heavy projectiles. For bullets the aerodynamic drag is an important phenomenon which requires to be accounted for while formulating its equations of motion. For a point-mass

**Table 2.** Data for the variation of $C_D$ with *Ma* of the G7 standard projectile

| Mach Number | $C_D$ |
|---|---|
| 0 | .120 |
| 0.5 | .119 |
| 0.6 | .119 |
| 0.7 | .120 |
| 0.8 | .124 |
| 0.9 | .146 |
| 0.95 | .205 |
| 1.0 | .380 |
| 1.05 | .404 |
| 1.1 | .401 |
| 1.2 | .388 |
| 1.3 | .373 |
| 1.4 | .358 |
| 1.5 | .344 |
| 1.6 | .332 |
| 1.8 | .312 |
| 2.0 | .298 |

assumption, such that the entire mass of the projectile is concentrated at a mathematical point, leads to the assumption that lift and Magnus forces are small everywhere along the trajectory in comparison to the drag force. Hence the aerodynamic drag and gravity are the only significant forces acting on the bullet.

The drag force coefficient ($C_D$) is the proportionality constant which relates the drag force experienced by a moving body to its area of presentation and its velocity. The drag force is always directed opposite to the velocity vector, irrespective of the direction the projectile is pointing in, hence the negative sign. If the long axis coincides with the velocity vector in zero-yaw flight, the drag force coefficient is only $C_{D0}$, the zero-yaw drag coefficient.

The aerodynamic drag vector is given by $\vec{F_D} = -\frac{1}{2}\rho S C_D V\vec{V}$, and the vector acceleration equation is given by:

$$\dot{V} = \frac{dV}{dt} = \dot{V_x}\hat{\imath} + \dot{V_y}\hat{\jmath} + \dot{V_z}\hat{k} = -\rho\frac{SC_D}{2m}.V\vec{V} + \vec{g},$$

where $\rho$ = density of the medium; $S$ = reference area/area of presentation; $C_D$ = drag force coefficient; $\vec{V}$ = velocity vector; $V$ = velocity magnitude; $\hat{\imath}$ = unit vector in the direction of the velocity.

Hence, the Point-Mass equations of motion are as follows:

$$\dot{V_x} = -C_D'VV_x$$
$$\dot{V_y} = -C_D'VV_y - g$$
$$\dot{V_z} = -C_D'VV_z$$

where,

$$C_D' = \rho\frac{SC_D}{2m};$$

$$V = \sqrt{V_x^2 + V_y^2 + V_z^2},$$

the scalar magnitude of the velocity.

Throughout the present work, a single sign convention and system of units has been used. The x, y and z axes are in a right-handed coordinate system, with the positive x-axis pointing downrange, the positive y-axis pointing vertically upwards and the positive z-axis pointing to the right across the range (Fig. 1).

The system of units used is the Imperial system or the Foot-Pound-Second (FPS) system of units due to convenience in translating available literature data for use in the computation. Hence all muzzle velocities are in feet per second, the acceleration due to gravity has an average value of 32.174 ft/s² and so forth.

***The Flat-Fire Approximation.*** The flat-fire approximation of the point-mass trajectory equations stems from the assumption that the components of velocity along the y and z axes during the entire flight of the bullet are much smaller in magnitude than the x-axis component. Thus,
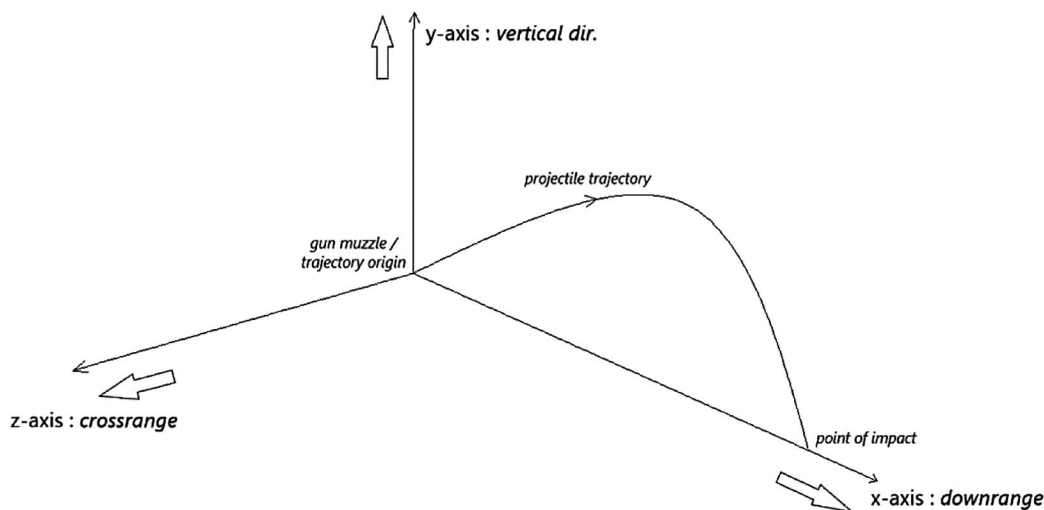
**Fig. 1.** System of axes for ballistic range [15].

$V_y$, $V_z$ << $V_x$, considering x-axis to be positive along the downrange direction. Thus, the scalar velocity magnitude V is approximated by $V_x$, which reduces the point-mass equations to the flat-fire trajectory equations, as follows:

$$\dot{V}_x = -C_D' V_x^2$$
$$\dot{V}_y = -C_D' V_x V_y$$
$$\dot{V}_z = -C_D' V_x V_z.$$

The equations from the analytical solution of the flat-fire trajectory considering a constant drag coefficient are:

$$r = \frac{V_{x_0}}{V_x} . k_1 = \frac{\rho S C_D}{2m}.$$

$$t = X.(r-1)/V_{x_0}.\ln(r).$$

$$\tan \varphi = \tan \varphi_0 - \frac{gt}{V_{x_0}}.\left[\frac{1}{2}(1+r)\right].$$

$$Y = Y_0 + X.\tan \varphi_0 -$$
$$- \frac{1}{2}gt^2\left[\frac{1}{2} + (r-1)^{-1} - (r-1)^{-2}.\ln(r)\right],$$

where the independent variable is the downrange distance $X$, time $t$ is the independent variable and $V_{x_0}$ = x-component of the muzzle velocity; $V_x$ = x-component of the instantenous velocity; $X$ = instantenous position of the point-mass along the x-axis; $Y$ = instantenous positin of the point-mass along the y-axis; $Y_0$ = y-component of the initial position of the point-mass; $\varphi_0$ = angle of firing,or the initial angle of inclination of the velocity vector; $\varphi$ = instantenous angle of inclination of the velocity vector.

The equation of motion along the z-axis is transformed to $\dot{V}_z = -C_D' V_x(V_z - W_z)$ in the presence of a crosswind, where $W_z$ is the crosswind velocity.

Mathematically, the deflection along the z-axis due to a crosswind is given by:

$$Z = W_z.\left(t - {}^X\!/_{V_{x_0}}\right),$$

where $t$ is the actual time of flight and $\left({}^X\!/_{V_{x_0}}\right)$ is the time in which the bullet will travel to the same range without any drag acting on it (i.e., in vacuum). The difference in these two flight times is called the lag time and the crosswind effectively can act on the bullet for this duration only.

## RESULTS AND DISCUSSION
### Aerodynamic Drag Coefficient

Sierra Bullets has published BC data for the range of their manufactured bullets and those were used in the script to get outputs of a $C_D$ vs. *Ma* plot up to 4.0 *Ma* with reference to the variation of $C_D$ with Mach number of the G7 standard projectile, and also an average $C_D$ was calculated for use in subsequent processes. BC data for B0 was extracted from McCoy [2].

The average $C_D$ calculated are reported in the sequence of increasing bullet weights (Table 3). The results for B0 to B6 are presented below.

Plots for the variation of the $C_D$ with *Ma* are given for bullets B0 and B6. The behaviour of the other bullets follows a similar trend (Fig. 2, 3).

It is observed that for the three 150 gr. Bullets (B1 — FMJBT; B2 — HPBT; B3 — SBT) there is a progressive increase in the average $C_D$. As the BC data indicates, in the subsonic regions, FMJBT has the highest BC among the three, and the lowest $C_D$ below 1800 fps. The HPBT however, has a lower drag coefficient than the FMJBT and the SBT in the supersonic regime.

**Table 3.** The calculated average $C_D$ and Sectional Density of bullets B0 to B6

| Bullet | Weight (grains) | Construction | Sectional Density (lbs./in$^2$) | $C_{Davg}$ |
|---|---|---|---|---|
| B0 | 147 | FMJ | 0.221 | 0.2915 |
| B1 | 150 | FMJ | 0.226 | 0.1508 |
| B2 | 150 | HPBT | 0.226 | 0.1599 |
| B3 | 150 | SBT | 0.226 | 0.1623 |
| B4 | 165 | SBT | 0.248 | 0.1569 |
| B5 | 168 | TMK | 0.253 | 0.1328 |
| B6 | 175 | HPBT | 0.264 | 0.1407 |

*Note:* FMJ — Full Metal Jacket; HPBT — Hollow Point Boattail; SBT — Spitzer Boattail (Soft-nosed); TMK — Tipped MatchKing [8].
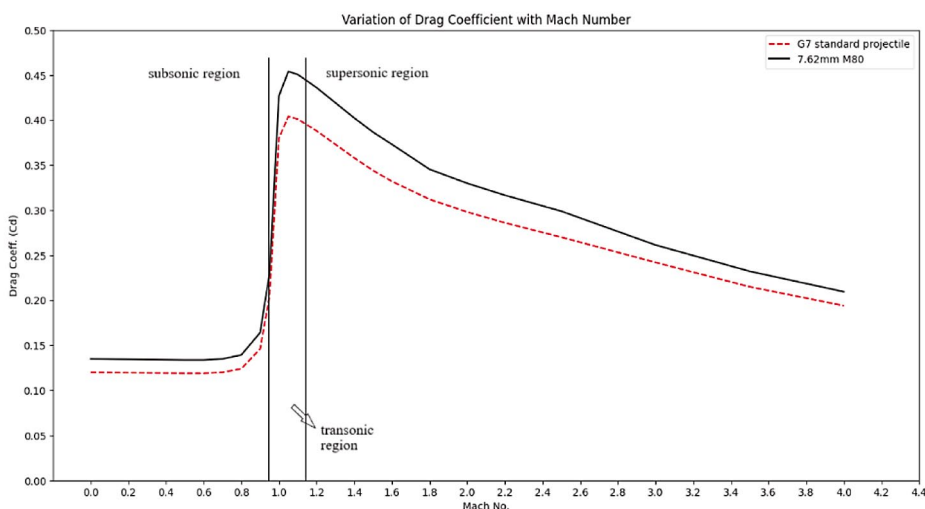


**Fig. 2.** $C_D$ vs. *Ma*, B0.
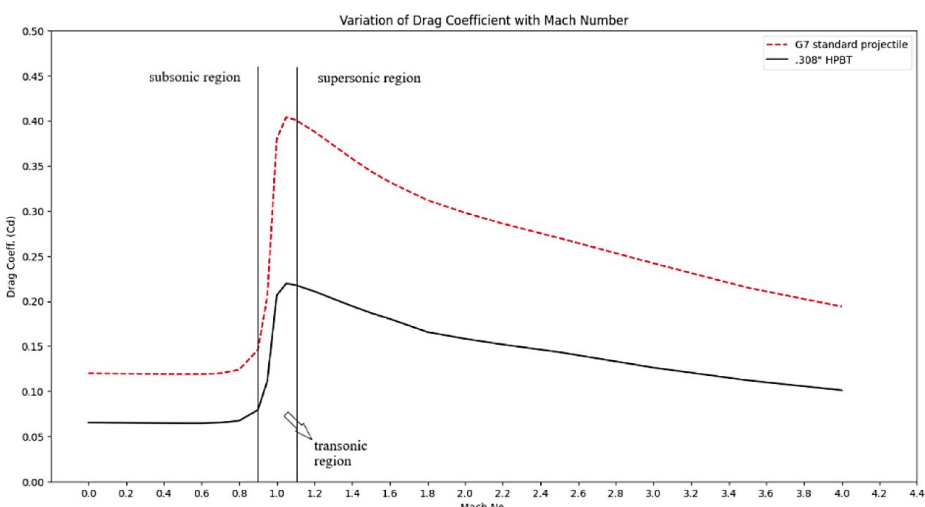


**Fig. 3.** $C_D$ vs. *Ma*, B6.

Of the six chosen Sierra bullets, it is evident that the drag coefficient shows a decreasing trend as the weight of the bullet increases and consequently the sectional density (150 gr. SBT (B3) [0.1623] → 165 gr. SBT (B4) [0.1569]). The 175 gr. Bullet should have the lowest $C_D$ along this trend. However, the lowest in the group is the 168 gr. TMK (B5) as there is a slight increase in the drag of the 175 gr. HPBT (B6) due to the hollow point.

The data for BCs for the bullet designated B0 has been extracted from McCoy where table of striking distance versus velocity is given for the 7.62 mm/.308" Ball M80. The variation in $C_D$ vs. *Ma* for B0 has been given in McCoy from actual live firing data by spark photography. The average $C_D$ for the 147 gr. M80 bullet is calculated to be 0.291. The plot shows that the form factor is greater than 1 w.r.t. the G7 standard. On the other hand, all the Sierra bullets have *i* values about 0.5.

## The Point-Mass Trajectory

Referring to the 2-d plot of point-mass trajectories above, with angle of firing 35° of the 7 bullets chosen for observation, it is seen that B0 with the highest $C_{Davg}$=0.291, has the shortest range, while B5 ($C_{Davg}$=0.1328) travels the farthest. Owing to the higher drag experienced by B0, its trajectory past its apogee is steeper and consequently its angle of impact is highest in the group at -77.263°. Similarly, B5 has the lowest angle of impact of -72.906° and B6 is very close at an angle of -73.008°. B0 to B6 show a sequence of increasing ranges as follows — B0, B3, B2, B1, B4, B6, B5 (Fig. 4; Table 4).

B2 trajectories are simulated at 20°, 30°, 35°, 45°, 50° angles of firing. It is seen that the range increases from 20° to 30° but a subsequent increase in the angle results in a higher apogee but a decreased range. To observe this crossing over of trajectories, more trajectories were plotted for firing at 15, 20, 25, 28, 30, 35, and 38 degrees (Fig. 5, 6; Table 5). The crossover trajectories are observed to start between 28° to 30°.
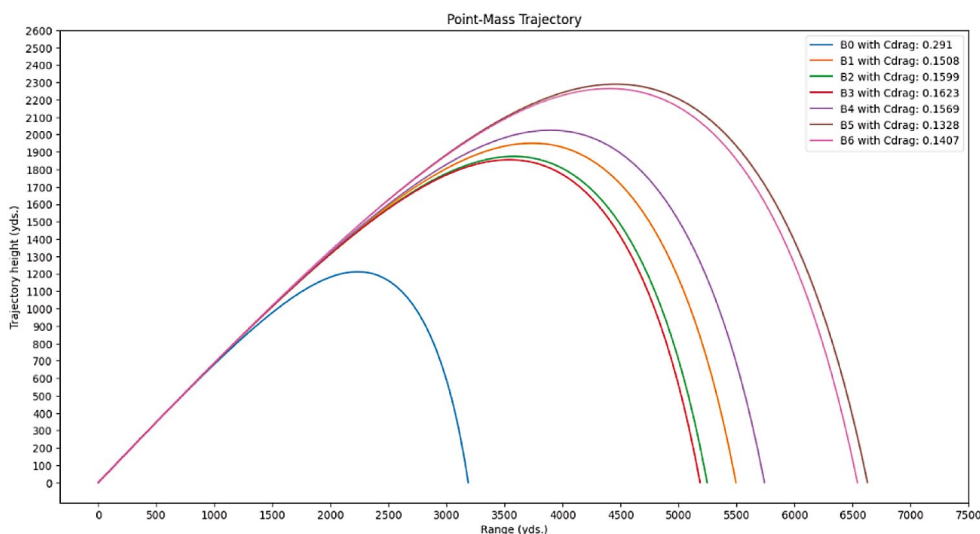


**Fig. 4.** Free-flight trajectory of bullets B0 to B6, fired at 35°.

**Table 4.** Trajectory simulation parameter outputs of B0 to B6 from the solution of 2-d Point-Mass equations of motion, $V_0$=2800 fps

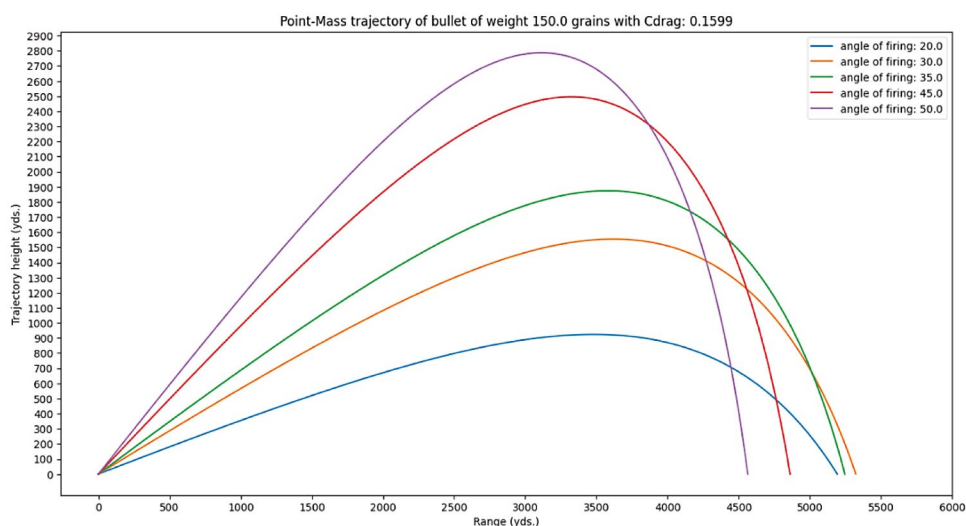| Bullet | Range (yards/metres) | Apogee (yards/metres) | Time of flight (seconds) |
|---|---|---|---|
| B0 | 3186.740/2913.955 | 1211.858/1108.123 | 28.82 |
| B1 | 5493.006/5022.804 | 1950.594/1783.623 | 36.73 |
| B2 | 5245.051/4796.074 | 1874.473/1714.018 | 35.99 |
| B3 | 5183.528/4739.818 | 1855.516/1696.684 | 35.80 |
| B4 | 5738.268/5247.072 | 2025.234/1851.874 | 37.44 |
| B5 | 6625.684/6058.525 | 2289.831/2093.821 | 39.87 |
| B6 | 6539.687/5979.889 | 2264.443/2070.606 | 39.65 |



**Fig. 5.** B2 fired at multiple angles (a).
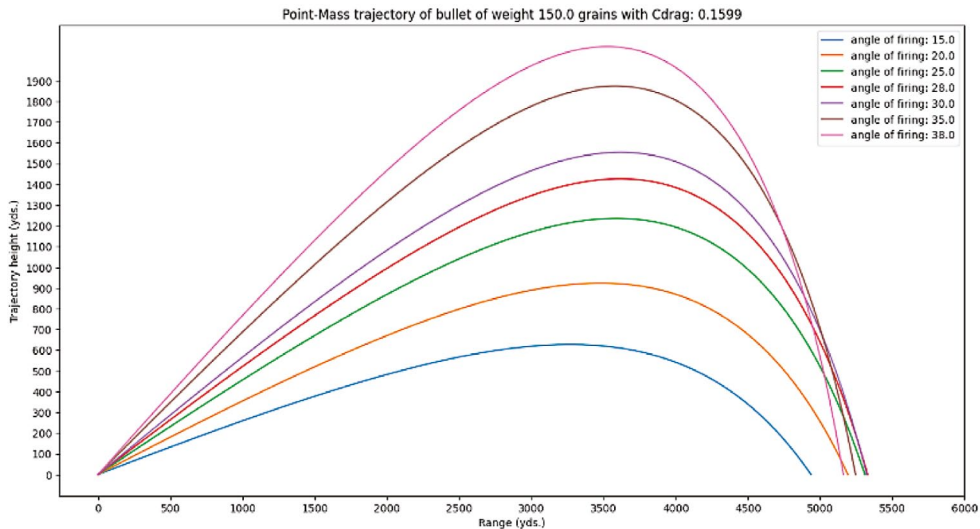
**Fig. 6.** B2 fired at multiple angles (b).

**Table 5.** Range of free flight of B2 when fired at different angles, $V_0$=2800 fps

| Bullet | Angle of firing (degrees) | Range (yards/meters) |
|--------|---------------------------|----------------------|
|        | 15                        | 4936.238/4513.696    |
|        | 20                        | 5191.294/4746.919    |
|        | 25                        | 5309.688/4855.178    |
|        | 28                        | 5328.453/4872.338    |
| B2     | 30                        | 5321.757/4866.215    |
|        | 35                        | 5245.051/4796.074    |
|        | 38                        | 5160.387/4718.657    |
|        | 45                        | 4860.199/4444.166    |
|        | 50                        | 4563.071/4172.472    |

Point-mass equations of motion were solved with a 3-dimensional wind vector as input to observe the effects of various directions of constant wind on the trajectory characteristics. Bullet B2 was projected with only a tailwind (+ve x-axis, 25fps) at 30°. It is seen that the tailwind extends the range by around 250 yards and the angle of impact is flattened to 67° from 70°. The time of flight is only increased by 0.1s while the trajectory height increases by 8 yards (Fig. 7).
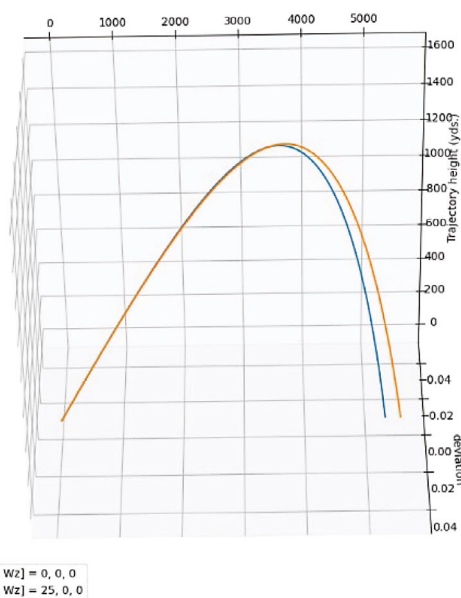


**Fig. 7.** B2 fired with no wind and only tailwind.

## Program Output

Wind = 0, 0, 0 the time of flight is 32.58 s the angle of impact is -70.22946346976369 degrees the range is: 5321.906787596593 yards the maximum height of the trajectory is: 1554.237484123316 yards the deflection in trajectory is: 0.0 yards Wind = 25, 0, 0 the time of flight is 32.68 s the angle of impact is -67.17979848766699 degrees the range is: 5574.052637946189 yards the maximum height of the trajectory is: 1562.7391482428018 yards the deflection in trajectory is: 0.0 yards

Further trajectory plots were generated for B3 with various combinations of wind vectors, as given below (Fig. 8; Table 6).

## Flat-Fire Trajectory

Flat-fire trajectory plots were generated for bullets B0 to B6 for a firing angle of 0.2° (12') with a muzzle velocity of 2800 fps (Fig. 9).

Similar to the point-mass trajectories, as expected, the lowest range is covered by B0, and the maximum by B5. The
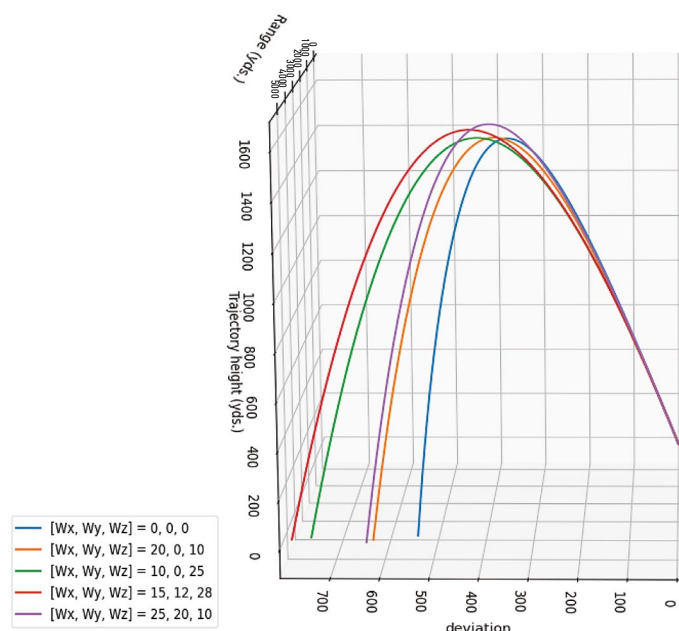


**Fig. 8.** B3 fired with multiple wind configurations (up-range view).

**Table 6.** B3 range and apogee for firing with various wind combinations

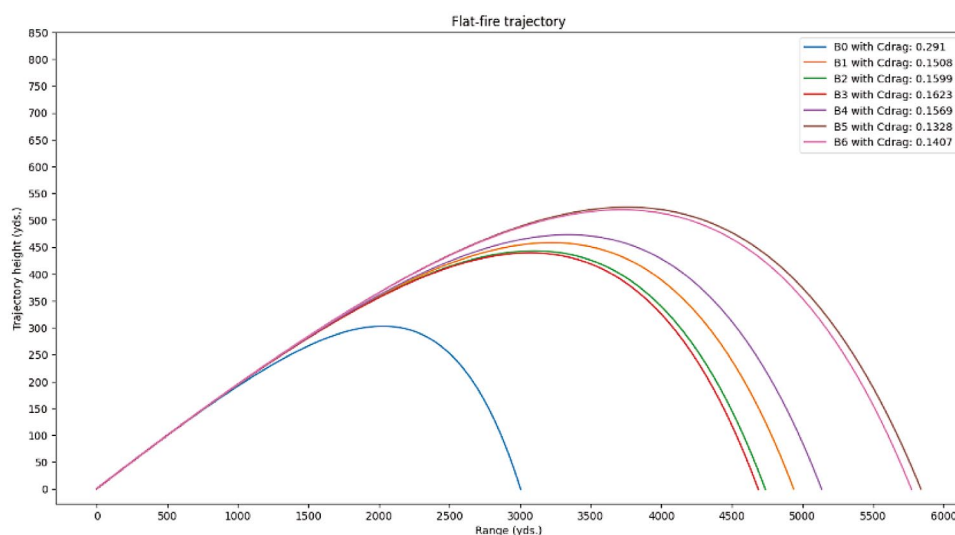| Bullet | $W_x$ (fps) | $W_y$ (fps) | $W_z$ (fps) | Range (yards/meters) | Apogee (yards/meters) | Deviation (yards/metres) |
|---|---|---|---|---|---|---|
|  | 0 | 0 | 0 | 5234.379/4786.316 | 1530.815/1399.777 | 528.79/483.52 |
|  | 20 | 0 | 10 | 5435.989/4970.668 | 1537.820/1406.182 | 617.96/565.06 |
| B3 | 10 | 0 | 25 | 5337.571/4880.675 | 1534.947/1403.555 | 745.86/682.01 |
|  | 15 | 12 | 28 | 5434.904/4969.676 | 1571.343/1436.836 | 784.40/717.25 |
|  | 25 | 20 | 10 | 5568.686/5092.006 | 1597.872/1461.094 | 630.43/576.46 |



**Fig. 9.** Flat-fire trajectory of bullets B0 thru B6.

**Table 7.** Flat-fire trajectory simulation parameter outputs of B0 to B6 fired at an elevation of 12', $V_0$=2800 fps

| Bullet | Range (yards/meters) | Apogee (yards/meters) | Time of flight (seconds) |
|--------|----------------------|-----------------------|--------------------------|
| B0 | 3003.67/2746.55 | 303.05/277.11 | 14.11 |
| B1 | 4937.00/4514.39 | 458.03/418.82 | 17.61 |
| B2 | 4737.00/4331.51 | 442.80/404.89 | 17.30 |
| B3 | 4687.00/4285.79 | 438.99/401.41 | 17.22 |
| B4 | 5135.34/4695.75 | 472.80/432.33 | 17.92 |
| B5 | 5838.67/5338.88 | 524.00/479.15 | 18.94 |
| B6 | 5772.00/5277.92 | 519.17/474.73 | 18.85 |

parameters of the trajectory obtained as the program output are given in Table 7.

Being fired at a low angle of elevation, the apogee of the trajectories are around 4 times shorter than when fired at 35°. The range of flights are not reduced to the same extent however, with B0 falling short by 183 yards when compared to its 3186.74 yards range when fired at 35°. Similarly, the ranges of B1 thru B6 fly shorter distances than when fired at 35°, but not to the magnitude of the shortened trajectory heights. The time of flight of the bullet is significantly shorter when compared to high angle of elevation firing, with the flat-fired bullet taking around half the time as it took when fired high at 35°.

One characteristic that is immediately evident is that unlike the crossover of trajectories at high-angles of fire, increasing the angles of firing from 0.05° to 0.2° causes a progressive increase in the range (Fig. 10; Table 8), which

is termed as 'rigid trajectory'. The change in elevation angle causes an increase in trajectory height directly in proportion to the range. The trajectory behaves as if it is rotating rigidly about the origin.

3-dimensional trajectory plots are also produced to visualise the deviation from the plane of firing due to a constant crosswind. Bullets B0 to B6 are projected at 0.2° with a simulated constant crosswind of 10 fps and 15 fps. The trajectory visualisations and related trajectory parameter outputs are given below (Fig. 11; Table 9).

## Study limitations and future scope

Since, a Ballistic Testing Range was unavailable for use, therefore, live firings of the 7.62 mm/.308" rounds could not be conducted. The actual free-flight trajectories could not be documented for validation against the simulated trajectories generated by the numerical solution of the equations of
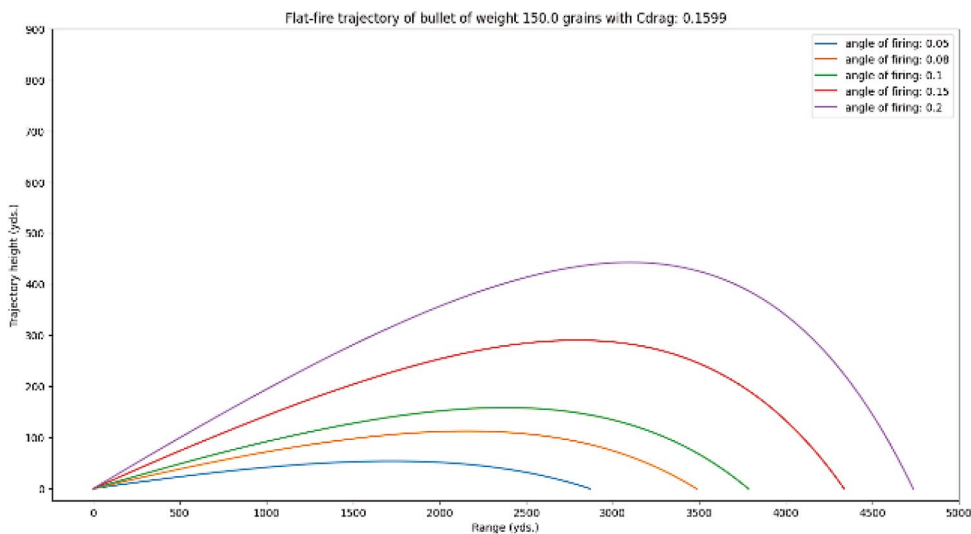


**Fig. 10.** B2 fired at multiple angles (flat-fire).

**Table 8.** Range of free flight for flat fire at multiple angles for bullets B2

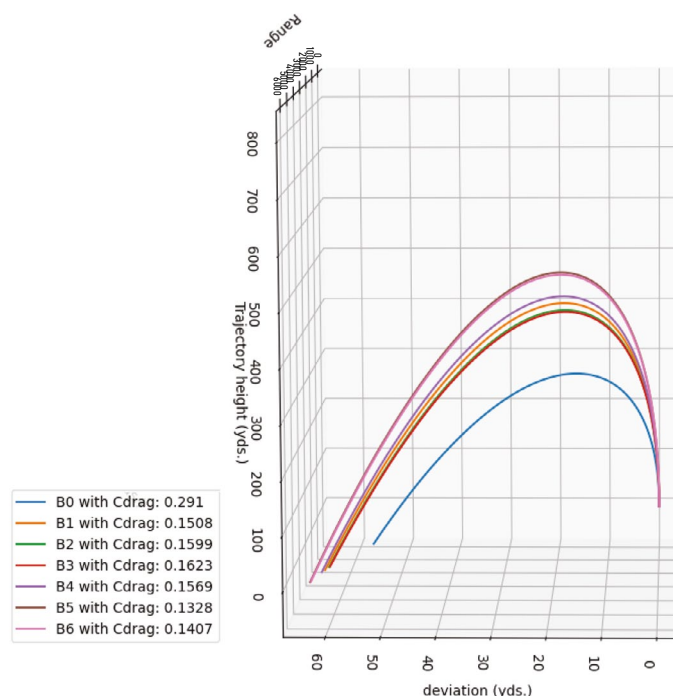| Bullet | Angle of firing (degrees/minutes) | Range (yards/meters) |
|--------|-----------------------------------|----------------------|
| | 0.05/3 | 2870.34/2624.63 |
| | 0.08/4.8 | 3485.34/3186.99 |
| B2 | 0.1/6 | 3783.67/3459.78 |
| | 0.15/9 | 4337.00/3965.75 |
| | 0.2/12 | 4737.00/4331.51 |

**Fig. 11.** Multiple trajectories at 15 fps crosswind (b: up-range view).

**Table 9.** Deflection in trajectory for B0 to B6 for two crosswind velocities

| Bullet | Deflection (yards/meters) | |
| --- | --- | --- |
| | $W_z$=10 fps | $W_z$=15 fps |
| B0 | 36.31/33.20 | 54.47/49.81 |
| B1 | 41.11/37.59 | 61.67/56.39 |
| B2 | 40.76/37.27 | 61.14/55.91 |
| B3 | 40.67/37.18 | 61.01/55.78 |
| B4 | 41.39/37.84 | 62.09/56.77 |
| B5 | 42.29/38.66 | 63.43/58.00 |
| B6 | 42.23/38.61 | 63.35/57.92 |

motion. The muzzle velocity used for the trajectory simulation is a uniform 2800 fps, however, a velocity measurement system would have allowed the author to simulate the trajectory for evaluation with the actual measured muzzle velocity as input into the program.

Furthermore, actual ballistic coefficients of the particular bullets could not be estimated for comparison and verification of the published data, the process of which requires multiple velocity measurement systems or doppler radar apparatus to measure near and far velocities of the bullet. High-speed photography of the firing would have allowed the estimation of the CD from data reduction. Moreover, CFD analysis could not be carried out for the estimation of the aerodynamic coefficients due to lack of expertise in handling CFD software such as ANSYS Fluent and the lack of actual bullet samples and data regarding geometric dimensions of the different bullets. An attempt at the solution of the 6-DoF equations of motion could not be carried out due to lack of academic expertise and experience in the field of ballistics and range work.

Further studies along the lines of this project can be carried out for the verification of the published BC data by various manufacturers for their products, rifle and handgun bullets alike. Trajectories for impact at short and intermediate ranges can be simulated, especially for the investigation of urban gunshot crime scenes involving firing at close ranges.

The drag coefficient can be calculated by scaling reference drag coefficient table by an appropriate form factor of the projectile. The form factor of a projectile can be theoretically calculated by using its geometric dimensions, as suggested by Savastre et al. (2020) [16] and previously by Surdu et al. (2015) [17]. Savastre et al. report that longer ballistic caps result in a low form factor/shape index and thus face a lower aerodynamic drag during flight. The usual method of calculating form factors of a bullet is by test firing a round to measure the ballistic coefficient across various velocity ranges, available in the form of compiled data published by manufacturers, such as one by Sierra Bullets [10]. Reddy et al. (2018) [18] reported their work on modelling of an AK-47 7.82 mm bullet to compute the $C_D$ at Mach 2 and the solution of a flat fire trajectory using C++ programming. Their result for the value of the drag coefficient has a 4% error from previously published data, and the simulated flat-fire trajectory

has a reported error of <0.01%. The authors have also investigated the effects of change in altitude on the range and terminal velocity of the bullet.

## CONCLUSION

This project presents the numerical solution of equations of motion of the Point-Mass model for a bullet fired from a gun to computationally simulate its trajectory. A group of seven 7.62 mm/.308" rifle bullets were chosen as samples to simulate free-flight trajectories. The programming language Python is well-equipped to carry out numerical solutions of systems of differential equations owing to its library of in-built functions which assists in writing an efficient script and reduces computational load.

This method of solution can be applied with suitable modifications in the field of forensic ballistics for the reconstruction of bullet trajectories and to form a conclusion based on the available evidence from a crime scene. Any forensic ballistic expert with an understanding of the fundamental principles of ballistics can apply this computational method to find a solution of the flight of a bullet and build an overview to a great extent of the crime scene layout from evidential data.

## ADDITIONAL INFORMATION

## REFERENCES

**1.** Warlow T.A. Firearms, the law, and forensic ballistics. 2nd ed. Boca Raton, Fla: CRC Press; 2005. 456 p.
**2.** McCoy R.L. Modern exterior ballistics: the launch and flight dynamics of symmetric projectiles. Rev. 2nd ed. Atglen, PA: Schiffer Pub; 2012.
**3.** 7.62X51 mm 147 Grain FMJ Lead Core M80 ball range grade ammunition. Available from: https://fedarm.com/product/7-62x51-308-win-147-grain-fmj-lead-core-m80-ball-range-grade-ammunition/. Accessed: Apr. 15, 2022.
**4.** 30 CALIBER/7.62MM 150 GR. FMJBT. Sierra Bullets. Available from: https://www.sierrabullets.com/product/30-caliber-7-62mm-150-gr-fmjbt/. Accessed: Apr. 15, 2022.
**5.** 30 CALIBER/7.62MM 150 GR. HPBT MATCHKING. Sierra Bullets. Available from: https://www.sierrabullets.com/product/30-caliber-7-62mm-150-gr-hpbt-matchking/. Accessed: Apr. 15, 2022.
**6.** 30 CALIBER/7.62MM 150 GR. SBT. Sierra Bullets. Available from: https://www.sierrabullets.com/product/30-caliber-7-62mm-150-gr-sbt/. Accessed: Apr. 15, 2022.
**7.** 30 CALIBER/7.62MM 165 GR. SBT. Sierra Bullets. Available from: https://www.sierrabullets.com/product/30-caliber-7-62mm-165-gr-sbt./ Accessed: Apr. 15, 2022.
**8.** 30 CALIBER/7.62MM 168 GR. TMK. Sierra Bullets. Available from: https://www.sierrabullets.com/product/30-caliber-7-62mm-168-gr-tmk/. Accessed: Apr. 15, 2022.
**9.** 30 CALIBER/7.62MM 175 GR. HPBT MATCHKING. Sierra Bullets. Available from: https://www.sierrabullets.com/product/30-caliber-7-62mm-175-gr-hpbt-matchking/. Accessed: Apr. 15, 2022.
**10.** Ballistic Coefficients. Sierra Bullets. Available from: https://www.sierrabullets.com/resources/ballistic-coefficients/. Accessed: May 06, 2022.
**11.** Courtney E., Morris C., Courtney M. Accurate measurements of free flight drag coefficients with amateur doppler radar. *arXiv*. 2016. Available from: http://arxiv.org/abs/1608.06500. Accessed: May 01, 2022.
**12.** Courtney E., Courtney A., Courtney M. Methods for accurate free flight measurement of drag coefficients. *arXiv*. 2015. Available from: http://arxiv.org/abs/1503.05504. Accessed: May 01, 2022.
**13.** Litz B. Applied ballistics for long-range shooting. 3rd ed. Cedar Springs, Michigan: Applied Ballistics LLC; 2015.
**14.** Litz B. Aerodynamic drag modelling for ballistics. Applied Ballistics; 2016.
**15.** Gangopadhyay S. System of axes for ballistic range. 2022.
**16.** Savastre A., Cârceanu I., Bolojan A. Theoretical evaluation of drag coefficient for different geometric configurations of ballistic caps for an experimental 30×165 mm AP-T projectile. *J Mil Technol*. 2020. Vol. 3, N 2. P. 37–42. doi: 10.32754/JMT.2020.2.06
**17.** Surdu G., Slamnoiu G., Sava A.C., Vedinas I. Comparative evaluation of projectile's drag coefficient using analytical and numerical methods. *Review of the Air Force Academy*. 2015. Vol. 1, N 28. P. 101.
**18.** Siva Krishna Reddy D., Padhy B.P., Reddy B.K. Flat-fire trajectory simulation of AK-47 assault rifle 7.82-mm Bullet / Vijayaraghavan L., Reddy K.H., Jameel Basha S.M., eds. Emerging trends in mechanical engineering. Singapore: Springer Singapore; 2020. P. 415–425. doi: 10.1007/978-981-32-9931-3_40

## AUTHORS' INFO

**\* Richa Rohatgi,** MSc, PhD, Assistant Professor, Forensic Science; Rohini, New Delhi, 110085, India;
ORCID: https://orcid.org/0000-0001-5514-953X; Scopus Author ID: 57189091058;
Google Scholar: https://scholar.google.com/citations?user=9oZKN5wAAAAJ&hl=en&oi=ao; e-mail: rrohatgi2020@gmail.com

**Soham Gangopadhyay,** Post Graduate Student, MSc Forensic Science

\* Corresponding author